An Ion Ejection Technique for the Study of Ion–Molecule Reactions with Ion Cyclotron Resonance Spectroscopy

J. L. BEAUCHAMP* AND JOHN T. ARMSTRONG†
Arthur Amos Noyes Laboratory of Chemical Physics, California Institute of Technology, Pasadena, California 91109‡
(Received 12 September 1968)

A novel technique involving a straightforward modification of an ion cyclotron resonance spectrometer has been developed which utilizes the excitation of the characteristic oscillatory motion of the ions, due to the trapping field, for ejecting ions from the cyclotron resonance cell. By pulsing the rf ejection field and referencing the detection system to the pulsing frequency, a spectrum of ions whose number density is modulated by the pulsed ejection field is obtained. This is directly applicable in studying ion–molecule reactions for the determination of product ion distributions, even when other processes, such as direct ionization or concurrent ion–molecule reactions, contribute to product ions of interest.

INTRODUCTION

An understanding of the chemistry of ions provides considerable insight into the phenomena in nature which involve the production and subsequent activity of ions in the gas phase. The study of ionization phenomena in the gas phase during the past decade has received considerable impetus from the development of specialized electronic instrumentation and vacuum technology, with ion cyclotron resonance being one of the more ingenious spectroscopic techniques devised for these investigations.

The motion of a charged particle in a uniform magnetic field is constrained to a circular orbit whose angular or cyclotron frequency depends only on the magnetic field strength and the ionic charge to mass ratio. When an rf electric field is applied normal to the direction of the magnetic field at the cyclotron frequency, an absorption of energy occurs which is readily observed by means of a marginal oscillator–detector, which is sensitive enough to permit direct observation of as few as *30 ions*. By trapping the ions for several milliseconds, it becomes possible to examine the effects of ion–neutral collisions at pressures below 10^{-3} Torr.[1,2] While an analysis of linewidths yields information concerning elastic processes,[1,2] the application of ion cyclotron resonance to the study of ion–molecule reactions is of principal interest.[3–6]

A variety of steady state[6] and transient[1] experiments permit the determination of ion–molecule reaction rate constants, with double resonance experiments being used to identify reactions and provide information regarding the variation rate constants with ion energy.[5,6]

Pulsed double resonance spectra are obtained by sweeping a pulsed irradiating field through the cyclotron frequencies corresponding to the possible reactant ions while monitoring the product ion of interest, with the marginal oscillator output fed to a phase sensitive detector referenced to the pulsing frequency. Ion–molecule reaction rate constants usually show at least a slight variation with ion energy, causing a change in the number density of product ions when the irradiating oscillator is switched on and off. The modulation information necessary for the marginal oscillator and phase sensitive detector to produce a signal is thus transmitted only through an ion–molecule reaction.

While double resonance experiments provide a means for identifying ion-molecule reactions, they do not in themselves facilitate the determination of product ion distributions. Consider the reaction

$$A^+ + B \xrightarrow{k_1} C^+ + D \qquad A^+ + B \xrightarrow{k_2} E^+ + F \qquad (1)$$

in which two ionic products, C^+ and E^+, are produced competitively from the reaction of A^+ with B. If processes such as direct ionization or concurrent ion–molecule reactions lead to the production of C^+ and E^+, then the individual rate constants k_1 and k_2 can be determined only by a rather detailed analysis,[7] or by performing experiments such as can be done with a tandem mass spectrometer in which the reactant A^+ can be selectively generated.[8,9] In ion cyclotron double resonance experiments, acceleration of A^+ with the irradiating field causes changes in the reaction rate constants k_1 and k_2 which are detected by observing concomitant changes in the

* Alfred P. Sloan fellow.
† National Science Foundation Undergraduate Research Participant (1968).
‡ Contribution No. 3748.
[1] R. A. Fluegge, Cornell Aeronautical Lab. Rep. No. UA-1854-P-1, U. S. Department of Commerce Clearing House for Federal Scientific and Technical Information, Washington, D. C.
[2] J. L. Beauchamp, J. Chem. Phys. 46, 1231 (1967).
[3] L. R. Anders, J. L. Beauchamp, R. C. Dunbar, and J. D. Baldeschwieler, J. Amer. Chem. Soc. 45, 1062 (1966).
[4] J. L. Beauchamp, L. R. Anders and J. D. Baldeschwieler, J. Amer. Chem. Soc. 89, 4569 (1967).
[5] J. L. Beauchamp and S. E. Buttrill, Jr., J. Chem. Phys. 48, 1783 (1968).
[6] M. T. Bowers, D. D. Elleman, and J. L. Beauchamp, J. Phys. Chem. 72, 3599 (1968).
[7] A. G. Harrison and J. M. S. Tait, Can. J. Chem. 40, 1986 (1962).
[8] J. H. Futrell and C. D. Miller, Rev. Sci. Instr. 37, 1521 (1966).
[9] T. F. Moran and L. Friedman, Rev. Sci. Instr. 38, 668 (1967).

Downloaded 21 Dec 2005 to 131.215.225.171. Redistribution subject to AIP license or copyright, see http://rsi.aip.org/rsi/copyright.jsp

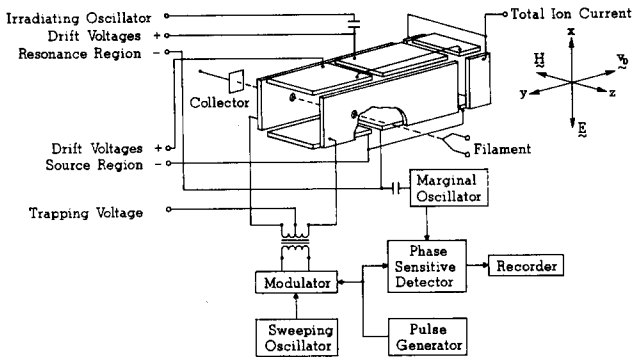

FIG. 1. Block diagram showing the modifications required to perform ion ejection experiments, including a cutaway view of the resonance cell.

production of C^+ and E^+. Thus while changes in k_1 and k_2 with ion energy can be examined, the absolute magnitudes of k_1 and k_2, or even their ratio, cannot be determined when other processes contribute to C^+ and E^+. This disadvantage could be circumvented if A^+ could be injected into, or selectively removed from, the cyclotron resonance cell. With the exception of spectrometers employing solenoid fields,[1] the geometry of the magnetic field employed does not allow for injection of a low energy ion beam into the apparatus. Irradiating fields sufficiently strong to eject A^+ have the undesirable effect of perturbing the marginal oscillator–detector. To obtain greater reactant selectivity in cyclotron resonance experiments, we have developed a novel technique which utilizes the excitation of the characteristic oscillatory motion of the ions, due to the trapping field, for ejecting ions from the cyclotron resonance cell. Sec. I describes the modification of the apparatus to perform these experiments. The nature of the electrostatic fields in the cell and their effect on the ion motion is discussed in Sec. II. The results of experiments designed to take advantage of this motion to eject ions from the cell are presented in Sec. III.

I. EXPERIMENTAL

The ion cyclotron resonance spectrometer used in this study is manufactured by Varian Associates (V-5900 series). The resonance cell employed is a standard design plug-in unit (Varian V-5950) whose basic features have been previously described.[4]

The modifications necessary to perform the ion ejection experiments, all external to the cell, are shown in the block diagram, Fig. 1, which includes a cutaway drawing of the resonance cell. Ions are formed by an electron beam accelerated in the direction of the primary magnetic field. The motion of the ions in the direction of the magnetic field is constrained by a trapping voltage applied to the side plates of the cell. With an electric field applied perpendicular to the direction of the magnetic field, the ions drift from the source region into the resonance region, the center of the ion orbit moving with constant velocity along an equipotential of the drift field. To facilitate matching the equipotential along which the ions drift in the source and resonance regions, the applied potentials which give rise to the drift fields are divided between the top and bottom plates of the cell, as indicated in Fig. 1. Separate potentials are applied in each region to isolate the rf fields used to irradiate and detect the ions in the resonance region. The net ion motion can thus be maintained in a plane centered between and parallel to the top and bottom plates of the cell. At the end of the cell, the trapping field is released permitting free motion of the ions in the direction of the magnetic field. The ions are thus collected and the total ion current measured. The spacing of the drift and trapping electrodes is 2.54 cm. The distance from the electron beam to the resonance region is 2.54 cm. The length of the resonance region is 6.35 cm.

As explained in Sec. II, the ions execute simple harmonic motion at frequency ω_T in the trapping field. The amplitude of these oscillations can be increased by applying an rf electric field (the ejection field) across the trapping plates, as indicated in Fig. 1. The ejection field is applied to the primary of a 2.8:1 surplus coupling transformer, with the trapping voltage being connected to the center tap of the secondary. A Hewlett–Packard 651B oscillator generates the ejection field which can be amplitude modulated (100%) using an FET switch triggered by Tektronix 160 series pulse generators. The output of the marginal oscillator is fed to a phase sensitive detector[10] which can be referenced either to the repetitive pulse of the Tektronix units, or to conventional modulation schemes such as field modulation.[4] Ejection of a particular ion from the cell can be ascertained by its absence from the field modulation spectrum, or it can be directly observed using the pulsed-ejection field.

The argon employed was obtained from Airco division of Union Carbide (purity > 99.9%). C_2D_4 (99% isotopic purity) was obtained from Merck, Sharpe, and Dohme of Canada. All other gases were obtained from Matheson (>99% purity). The background pressure in the spectrometer was less than 10^{-8} Torr prior to performing each experiment.

II. ANALYSIS OF ELECTROSTATIC FIELDS AND ION MOTION IN THE CYCLOTRON RESONANCE CELL

With the drift electrodes at ground, the potential applied to the trapping plates gives rise to a quadrupole field near the center of the cell. The space potential can

[10] Princeton Applied Research, model HR-8.

Downloaded 21 Dec 2005 to 131.215.225.171. Redistribution subject to AIP license or copyright, see http://rsi.aip.org/rsi/copyright.jsp

be approximated by

$$V=V_0+C(z^2-x^2), \tag{2}$$

where V_0 is the potential at the center of the cell and the constant C is chosen to match the boundary conditions best. The origin of the coordinate system indicated in Fig. 1 is taken at the center of the electron beam, midway between the trapping electrodes. By symmetry, $V_0=\frac{1}{2}V_T$ when V_T is the applied trapping voltage. If d is the spacing between the trapping electrodes, and Eq. (2) gives the correct potential at $x=0$ and $z=\pm d/2$, then

$$V=V_T[\tfrac{1}{2}+(2/d^2)(z^2-x^2)]. \tag{3}$$

The quadratic behavior of the space-dependent part of the potential described by Eq. (3) was confirmed by supplying appropriate voltages to silver electrodes painted on uniform resistance paper in accordance with the cell geometry. As shown in Fig. 2, a plot of $V-V_0$ against z^2 with $x=0$ is fairly linear near the center of the cell and deviates somewhat near the trapping electrode, the position of which is indicated by the broken vertical line. The effect of applying a drift voltage to the top plate of the cell is to reduce the coefficient of the z^2 term in Eq. (2) without appreciably involving higher order terms in the description of the potential (see Fig. 2). The effect of the trapping electrodes on the drift field was investigated for several potential configurations. In each case the measured field at the center of the cell was $80\pm1\%$ of the value given by V_D/d where V_D is the applied drift voltage.

The x and z components of the electric field near the center of the cell derived from the potential given by Eq. (3) and including the idealized drift field are

$$E_x=4xV_T/d^2+V_D/d \tag{4}$$

and

$$E_z=-4zV_T/d^2. \tag{5}$$

The drift field contribution to E_x gives rise to a drift velocity[11]

$$v_D=cV_D/dH, \tag{6}$$

whose direction is perpendicular to the magnetic and electric fields, as indicated in Fig. 1. The remaining contributions to the electric fields have two effects. The first is to cause a shift in the cyclotron resonance frequency ω_c to a new effective value ω_{eff} which can be calculated as follows[12]: The equation of motion for the ion velocity $\mathbf{v}$

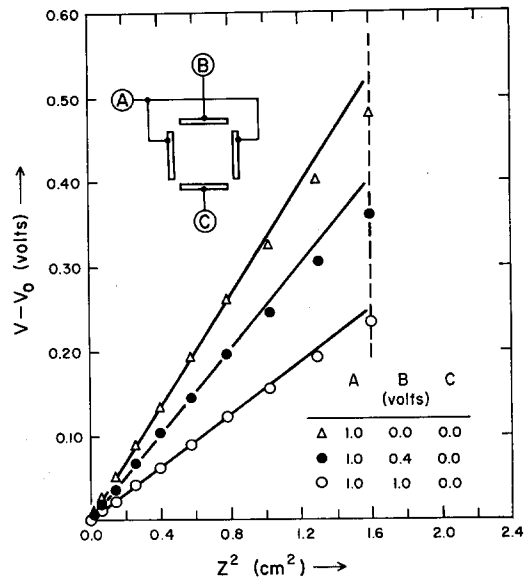

FIG. 2. Verification of the predominance of the quadratic term in the z component of the electric field in the cyclotron resonance cell for several combinations of trapping and drift voltages. V_0 represents the space potential at the center of the cell. The broken vertical line indicates the extension of the trapping electrode.

is given by

$$\frac{d\mathbf{v}}{dt}=\frac{q}{m}\left(\mathbf{E}+\frac{\mathbf{v}\times\mathbf{H}}{c}\right), \tag{7}$$

which has the components in the x–y plane,

$$dv_x/dt=4_qxV_T/md^2+\omega_cv_y \tag{8}$$

and

$$dv_y/dt=-\omega_cv_x, \tag{9}$$

where

$$\omega_c=qH/mc. \tag{10}$$

Differentiating Eq. (8) with respect to time yields

$$\frac{d^2v_x}{dt^2}=\frac{4qV_Tv_x}{md^2}+\omega_c\frac{dv_y}{dt}$$
$$=-(\omega_c^2-4qV_T/md^2)v_x, \tag{11}$$

which represents harmonic motion in v_x at a frequency

$$\omega_{\text{eff}}=(\omega_c^2-4qV_T/md^2)^{\frac{1}{2}}$$
$$\cong\omega_c(1-\omega_T^2/2\omega_c^2), \tag{12}$$

where, as shown below,

$$\omega_T=(4qV_T/md^2)^{\frac{1}{2}} \tag{13}$$

is a frequency characteristic of ion motion in the trapping field. Thus, to maintain resonance conditions at a fixed observing frequency, an increase in trapping potential must be compensated for by a corresponding linear increase in the magnetic field strength.

[11] W. P. Allis, in *Handbuch der Physik*, S. Flügge, Ed. (Springer-Verlag, Berlin, 1956), Vol. 21, p. 384.

[12] The effect of trapping fields on the cyclotron resonance frequency in an omegatron has been previously elucidated [H. Sommer, H. A. Thomas, and J. A. Hipple, Phys. Rev. **82**, 697 (1951)]. The treatment given this phenomenon above ascribes to the geometry of the resonance cell used in the present experiments.

Downloaded 21 Dec 2005 to 131.215.225.171. Redistribution subject to AIP license or copyright, see http://rsi.aip.org/rsi/copyright.jsp

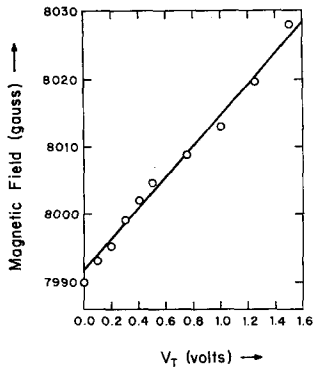

FIG. 3. Shift in magnetic field with trapping voltage required to maintain resonance conditions for Ar^+ at a fixed frequency (304.9 kHz).

The second effect which the electric fields derived from the trapping potential have on the ion motion is to establish an oscillation in the direction of the primary magnetic field. The component of Eq. (7) in the z direction becomes

$$dv_z/dt = -(4qV_T/md^2)z = -\omega_T^2 z, \tag{14}$$

which has the solution

$$v_z(t) = v_z(0)\cos(\omega_T t) - z(0)\sin(\omega_T t), \tag{15}$$

where $v_z(0)$ and $z(0)$ are the velocity and position of the ion along the z axis, respectively, at the time of formation. The amplitude of this oscillatory motion can be increased by applying an rf voltage V_{rf} at frequency $\omega=\omega_T$ across the trapping electrodes. The equation of motion becomes

$$d^2z/dt^2 = -\omega_T^2 z + qE_{rf}\sin\omega t/m, \tag{16}$$

where $E_{rf}=V_{rf}/d$. Taking initial conditions for the ion motion as

$$z(0)=0 \tag{17a}$$

and

$$dz(t)/dt|_{t=0}=0 \tag{17b}$$

leads to the solution

$$z(t) = (qE_{rf}/m\omega_T) \times\{[\omega_T\sin(\omega t) - \omega\sin(\omega_T t)]/(\omega_T^2-\omega^2)\}. \tag{18}$$

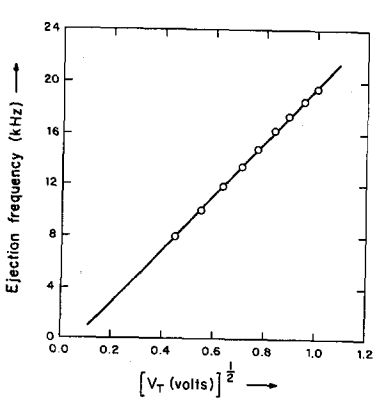

FIG. 4. Verification of the linear variation of the ejection field frequency with the square root of trapping voltage for Ar^+.

At resonance ($\omega=\omega_T$), Eq. (18) reduces to

$$z(t)|_{\omega=\omega_T} = (qE_{rf}/2m\omega_T)\{t\cos(\omega_T t) - \sin(\omega_T t)/\omega_T\}. \tag{19}$$

For $t\gg(\omega_T)^{-1}$, the second term in Eq. (19) can be neglected. The time required to eject an ion from the cell, which occurs when $z(t)=\frac{1}{2}d$, is given by

$$\tau_e = m\omega_T d/qE_{rf}. \tag{20}$$

III. APPLICATIONS OF THE ION EJECTION TECHNIQUE

The shift in the resonant magnetic field with trapping voltage at fixed observing frequency (304.9 kHz) is given in Fig. 3 for argon ions with drift voltages of 0.68 V in the source and resonance regions. The slope of the straight line in Fig. 3 yields a shift of 23±1 G/V. The calculated shift, using Eq. (11), is 16.3 G/V.

In practical units Eq. (12) yields

$$\omega_T/2\pi = 123.0(V_T/m)^{\frac{1}{2}}\text{ kHz}, \tag{21}$$

where V_T is in practical volts and m is in atomic mass units. For argon ions with $V_T=1.0$ V, Eq. (21) gives $\omega_T/2\pi=19.4$ kHz. At this trapping voltage and with drift voltages of 0.68 V in the source and resonance regions, applying the ejection field causes a decrease in the Ar^+ single resonance absorption monitored using field modulation, with the maximum effect occurring at a frequency of 20.0 kHz. A plot of the experimental ejection frequency vs the square root of the applied trapping voltage is shown in Fig. 4, the observed linearity confirming the relation delineated by Eq. (13). As described above, by pulsing the ejection field and referencing the detection scheme to the pulsing frequency, the ions ejected from the cell can be directly observed by sweeping the magnetic field. Such a spectrum, obtained with $V_T=1.0$ V, drift voltages in the source and resonance regions of 0.60 V, $\omega/2\pi=20.0$ kHz, and $V_{rf}=0.063$ V, is shown in the inset of Fig. 5. The $m/e=40$ (Ar^+) intensity in the pulsed ejection spectrum is given in Fig. 5 as a function of V_{rf}. Below 0.01 V no appreciable ejection of Ar^+ occurs. Above 0.01 V the intensity increases, reaching a maximum at $V_{rf}=0.05$ V which corresponds to complete ejection of Ar^+. With $\omega_T/2\pi=19.4$ kHz, the second term in Eq. (19) can be neglected for times long compared to ω_T^{-1} or 8.2×10^{-6} sec. From Eq. (20) the time required to eject Ar^+ with $V_{rf}=0.05$ V is 6.5×10^{-4} sec. It requires a calculated time of 8.5×10^{-4} sec for the ions to drift from the electron beam to the juncture of the source and resonance regions. The ions are thus ejected before entering the resonance region.

The mass resolution of the ion ejection technique can be experimentally determined by monitoring the intensity of a peak in the pulsed ejection spectrum and sweeping the ejection field frequency. With other conditions identi-

Downloaded 21 Dec 2005 to 131.215.225.171. Redistribution subject to AIP license or copyright, see http://rsi.aip.org/rsi/copyright.jsp

TABLE I. Product distributions from the reaction of H_3^+ with cyclopropane.

Product		Product distribution[a]	
m/e	Ion species	Ion cyclotron resonance ion ejection technique	Tandem mass spectrometer[b]
43	$C_3H_7^+$	15	0
42	$C_3H_6^+$	5	100
41	$C_3H_5^+$	100	52
40	$C_3H_4^+$	0	14
39	$C_3H_3^+$	6	28

[a] Major product taken as 100.
[b] Data from Ref. 12. Primary ion energy ~5 eV with 7.1 Å² cross section reported for production of $C_3H_6^+$.

cal to those employed to obtain the data in Fig. 5, this is shown for Ar^+ in Fig. 6 with $V_{rf}=0.063$ V. The full width at half-height of the resonance centered at 20 kHz in Fig. 6 is 3.0 kHz, which corresponds to 10 amu or a resolution, expressed as $M/\Delta M$, of 4.0. The origins of the small peak at 30 kHz and the notch in the resonance at 20 kHz were not ascertained. At higher values of V_{rf} the resonance at 20 kHz becomes broad with a flat top, corresponding to total ejection of Ar^+ over a wide range of ejection frequencies. Low trapping voltages and high drift voltages lead in general to poorer resolution. A resolution as high as 7 has been obtained with a 1:1 mixture of C_2H_4 and C_2D_4. With a nominal electron energy of 14.0 eV at 10^{-6} Torr only $C_2H_4^+$ and $C_2D_4^+$ are observed in the single resonance spectrum obtained with field modulation [Fig. 7(a)]. With a trapping voltage of 1.2 V and drift voltages of 0.88 and 0.12 V in the source and resonance regions of the cell, respectively, $C_2D_4^+$ can be totally removed from the single resonance spectrum at an ejection frequency of 24.4 kHz without measurably perturbing the $C_2H_4^+$ intensity [(Fig. 7(b)]. The calculated value of the ejection frequency [Eq. (21)] is 23.8 kHz, in good agreement with the experimental value.

With the limited resolution presently available, the ion ejection technique is best suited for studying the reactions of light ions such as H_3^+. To exemplify this application a 100:1 mixture of H_2 and cyclopropane was prepared. In this mixture the reaction

$$H_2^+ + H_2 \rightarrow H_3^+ + H \qquad (22)$$

leads to the production of H_3^+, which sustains several energy relaxing collisions with H_2 before undergoing proton transfer to cyclopropane,

$$H_3^+ + C_3H_6 \rightarrow H_2 + [C_3H_7^+]^*, \qquad (23)$$

a reaction sufficiently exothermic to lead to the decomposition of the excited product if collisional stabilization does not occur.[13,14]

[13] J. J. Leventhal and L. Friedman, J. Chem. Phys. 48, 1559 (1968).
[14] P. Ausloos and S. G. Lias, Discussions Faraday Soc. 39, 36 (1965).

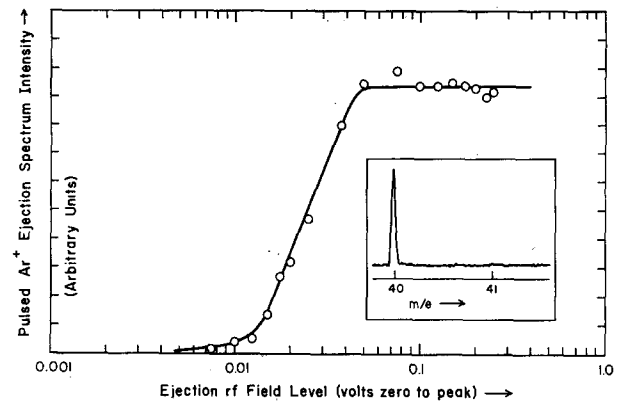

FIG. 5. Variation of pulsed Ar^+ ejection spectrum intensity with ejection rf voltage at 1.0 V trapping. Inset shows a typical pulsed Ar^+ ejection spectrum obtained by sweeping the magnetic field with an rf voltage of 0.063 V.

Figure 8(a) presents the single resonance spectrum in the region between $m/e=39$ and $m/e=43$ obtained with the H_2–cyclopropane mixture at 10^{-4} Torr and 40 eV electron energy. Field modulation gives the derivative presentation. As has been previously noted, high ion densities can cause a shift in the cyclotron resonance frequency[1,12] and distort the single resonance line shape.[1,4] Thus at high ion densities, periodically pulsing an appreciable fraction of the ions out of the cell can give rise to a frequency modulated signal observed at the output of the phase sensitive detector referenced to the pulsing frequency. Such a pulsed ion ejection spectrum, obtained with a total ion current $\gg 2\times10^{-11}$ A, is shown in Fig. 8(b). At lower ion densities (total ion current $<2\times10^{-11}$ A), the desired pulsed H_3^+ ejection spectrum is observed, displaying the products of the reaction of H_3^+ with cyclopropane [Fig. 8(b)]. The observed product distribution is given in Table I. The balance of the ionic species apparent in Fig. 8(a), the single resonance spectrum, are generated either by direct electron impact or from reactions of cyclopropane with H_2^+.

The distribution of C_3 products obtained by impacting H_3^+ on cyclopropane at a nominal ion energy of ~5 eV in a tandem mass spectrometer is included in Table I.[13] The

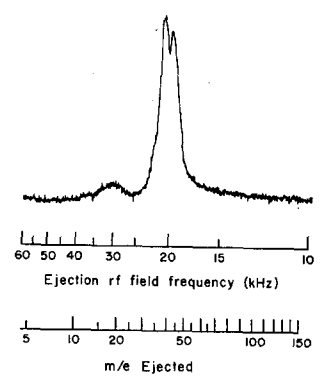

FIG. 6. Intensity of $m/e=40$ peak in the pulsed Ar^+ ejection spectrum (see inset Fig. 5) obtained by sweeping the ejection rf field frequency at a level of 0.063 V with 1.0 V trapping. The ejection rf field frequency has been converted to an equivalent m/e ejected using Eq. (21) in the text.

Downloaded 21 Dec 2005 to 131.215.225.171. Redistribution subject to AIP license or copyright, see http://rsi.aip.org/rsi/copyright.jsp

tandem mass spectrometer results are at considerable variance with the cyclotron resonance pulsed ion ejection results. The latter technique does not suffer from discrimination effects which might occur in the sampling of product ions in the tandem mass spectrometer. More important, however, are the different reactant ion energies employed in the two experiments. In the cyclotron resonance apparatus, the reactant ion energy is near thermal and more than two orders of magnitude less than the ~5 eV ion energy employed in the tandem mass spectrometer. If this is the case, then from Table I the relative importance of the processes

$$H_3^+ + C_3H_6 \rightarrow C_3H_6^+ + H_2 + H \quad (24)$$

and

$$H_3^+ + C_3H_6 \rightarrow C_3H_5^+ + 2H_2 \quad (25)$$

appears to depend on the reactant ion energy. Double resonance experiments confirm this conjecture, indicating that with increasing ion energy the rate of reaction (25) decreases considerably while the rate of the net charge exchange process [reaction (24)] increases slightly.

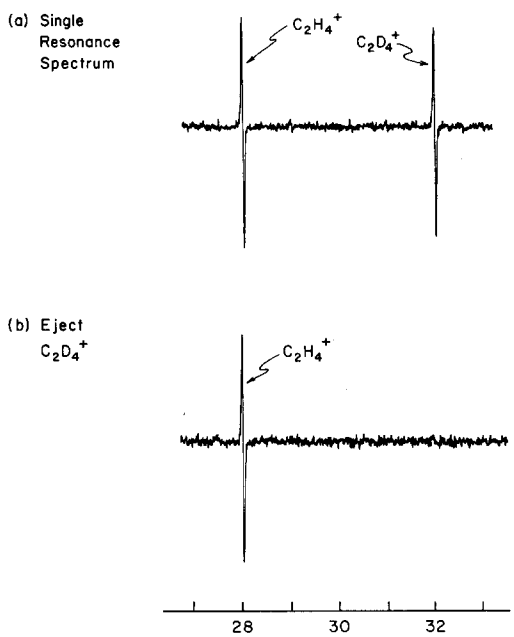

FIG. 7. (a) Single resonance spectrum of a 1:1 mixture of C_2H_4 and C_2D_4 at 14 eV electron energy and 10^{-6} Torr. (b) Repeat of single resonance spectrum with simultaneous ejection of $C_2D_4^+$ at 24.4 kHz with 1.2 V trapping.

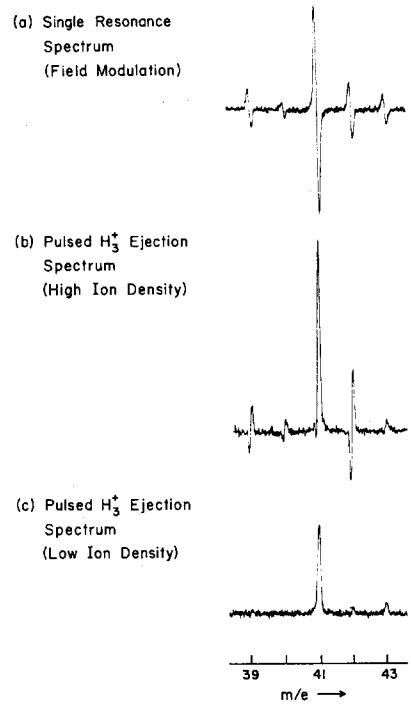

FIG. 8. (a) Single resonance spectrum of the $m/e=39$ to $m/e=43$ region of a 100:1 mixture of H_2 and cyclopropane at 40 eV electron energy and 10^{-4} Torr. Under these conditions, no other ions are observed between $m/e=44$ and $m/e=70$. (b) Pulsed H_3^+ ejection spectrum obtained with high ion densities, causing a frequency modulation and subsequent detection of all ionic species present. (c) Pulsed H_3^+ ejection spectrum at low ion densities, displaying the products of the reaction of H_3^+ with cyclopropane.

IV. DISCUSSION

It is evident that the ion ejection technique comprises a useful addition to the ion cyclotron resonance techniques already available for the study of ion–molecule reactions. It directly complements double resonance experiments, permitting the determination of product distributions as well as their partitioning with ion energy. While, as noted in the previous section, it is best suited for studying the reactions of light ions, improvement of the electric field distribution by appropriate changes in the electrode configurations as well as operation at higher trapping voltages may significantly extend the usefulness of the technique.

ACKNOWLEDGMENTS

The authors wish to acknowledge the assistance of John Henigman in performing circuit modifications. One of us (J. T. A.) wishes to thank the National Science Foundation for financial support. This work has been supported by the Atomic Energy Commission under Contract No. AT(04-3)-757.

Downloaded 21 Dec 2005 to 131.215.225.171. Redistribution subject to AIP license or copyright, see http://rsi.aip.org/rsi/copyright.jsp